ACCOUNTS of chemical research

Article

Cite This: Acc. Chem. Res. 2019, 52, 585−595

pubs.acs.org/accounts

# Artificial Metalloenzymes Based on the Biotin−Streptavidin Technology: Enzymatic Cascades and Directed Evolution

*Published as part of the Accounts of Chemical Research special issue "Artificial Metalloenzymes and Abiological Catalysis of Metalloenzymes".*

Alexandria Deliz Liang,[‡] Joan Serrano-Plana,[‡] Ryan L. Peterson,[‡] and Thomas R. Ward*

Department of Chemistry, University of Basel, BPR1096, Mattenstrasse 24a, CH-4058 Basel, Switzerland

**CONSPECTUS:** Artificial metalloenzymes (ArMs) result from anchoring a metal-containing moiety within a macromolecular scaffold (protein or oligonucleotide). The resulting hybrid catalyst combines attractive features of both homogeneous catalysts and enzymes. This strategy includes the possibility of optimizing the reaction by both chemical (catalyst design) and genetic means leading to achievement of a novel degree of (enantio)selectivity, broadening of the substrate scope, or increased activity, among others. In the past 20 years, the Ward group has exploited, among others, the biotin−(strept)avidin technology to localize a catalytic moiety within a well-defined protein environment. Streptavidin has proven versatile for the implementation of ArMs as it offers the following features: (i) it is an extremely robust protein scaffold, amenable to extensive genetic manipulation and mishandling, (ii) it can be expressed in *E. coli* to very high titers (up to >8 g·L$^{-1}$ in fed-batch cultures), and (iii) the cavity surrounding the biotinylated cofactor is commensurate with the size of a typical metal-catalyzed transition state. Relying on a chemogenetic optimization strategy, varying the orientation and the nature of the biotinylated cofactor within genetically engineered streptavidin, 12 reactions have been reported by the Ward group thus far. Recent efforts within our group have focused on extending the ArM technology to create complex systems for integration into biological cascade reactions and *in vivo*.

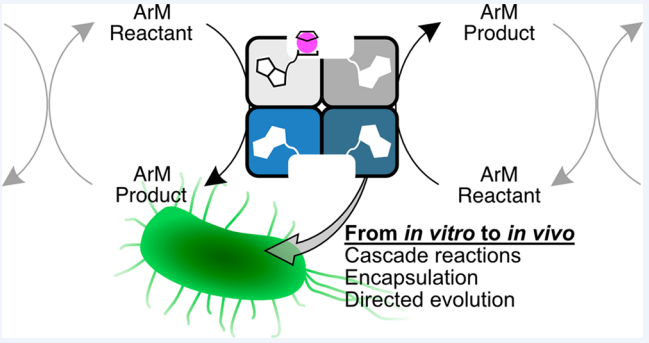


With the long-term goal of complementing *in vivo* natural enzymes with ArMs, we summarize herein three complementary research lines: (i) With the aim of mimicking complex cross-regulation mechanisms prevalent in metabolism, we have engineered enzyme cascades, including cross-regulated reactions, that rely on ArMs. These efforts highlight the remarkable (bio)compatibility and complementarity of ArMs with natural enzymes. (ii) Additionally, multiple-turnover catalysis in the cytoplasm of aerobic organisms was achieved with ArMs that are compatible with a glutathione-rich environment. This feat is demonstrated in HEK-293T cells that are engineered with a gene switch that is upregulated by an ArM equipped with a cell-penetrating module. (iii) Finally, ArMs offer the fascinating prospect of "endowing organometallic chemistry with a genetic memory." With this goal in mind, we have identified *E. coli*'s periplasmic space and surface display to compartmentalize an ArM, while maintaining the critical phenotype−genotype linkage. This strategy offers a straightforward means to optimize by directed evolution the catalytic performance of ArMs. Five reactions have been optimized following these compartmentalization strategies: ruthenium-catalyzed olefin metathesis, ruthenium-catalyzed deallylation, iridium-catalyzed transfer hydrogenation, dirhodium-catalyzed cyclopropanation and carbene insertion in C−H bonds. Importantly, >100 turnovers were achieved with ArMs in *E. coli* whole cells, highlighting the multiple turnover catalytic nature of these systems.

## 1. INTRODUCTION

Biology relies on a set of bioavailable elements and cofactors to catalyze a variety of chemical transformations. Biosynthesis is fine-tuned and regulated, allowing for multistep synthesis without the need for isolation of intermediates or protecting groups. In contrast, chemists are able to access non-bioavailable elements and molecules to develop catalysts. Multistep synthesis, however, often requires isolation of intermediates and use of protecting groups. Merging features of synthetic and biological catalysts could provide benefits for both biology and chemistry. Inserting synthetic catalysts into biological systems could expand the repertoire of reactions available in biology, giving access to new biocatalysts. Additionally, instilling catalysts with regulatory features prevalent in biology may enable cascades that are often not possible with synthetic catalysts. Introduction of catalysts into a biological context can be challenging for several reasons: (i)

Received: December 5, 2018
Published: February 8, 2019






DOI: 10.1021/acs.accounts.8b00618
Acc. Chem. Res. 2019, 52, 585−595

**Scheme 1. Enzyme Cascades Using ATHases**[a]

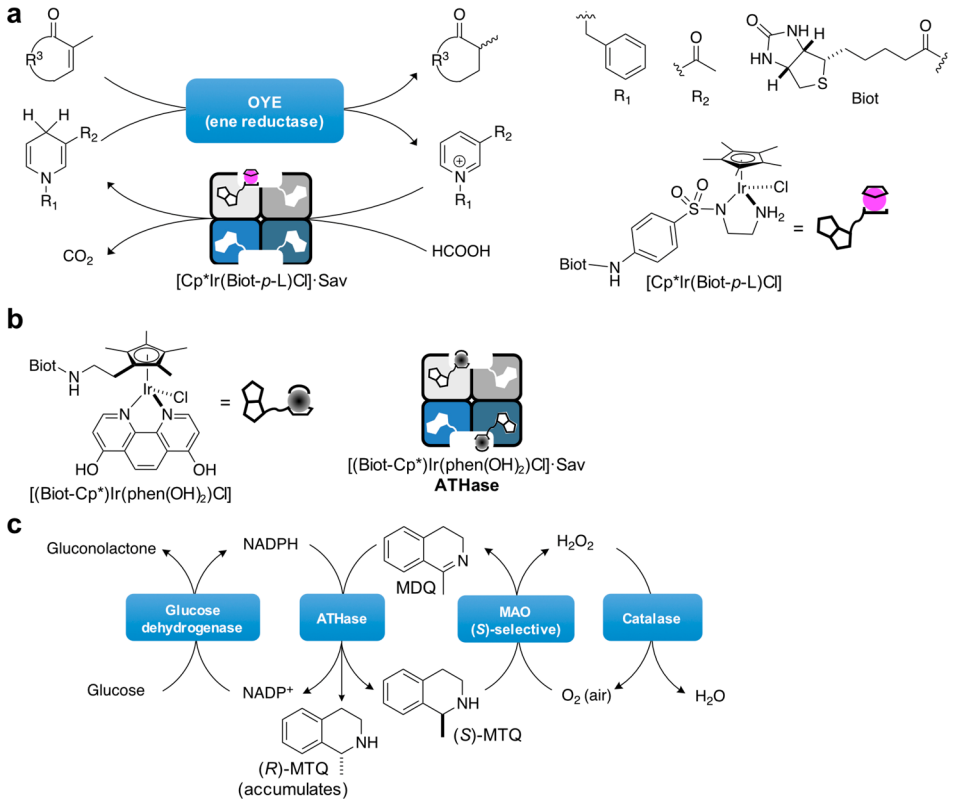


[a](a) Catalytic reduction of enones by ene reductase and catalytic $NAD^+$ regeneration by [Cp*Ir(Biot-*p*-L)Cl]·SAV. (b) Cofactor and corresponding ATHase: [(Biot-Cp*)Ir(phen$(OH)_2$)Cl]·SAV. (c) Four enzyme cascade for the reduction of cyclic imines using glucose as terminal reductant.

homogeneous catalysts are often intolerant toward oxygen, water, or both, (ii) cross-reactivity of synthetic catalysts and biomolecules can lead to mutual deactivation,[1] and (iii) synthetic catalysts often perform best in organic solvents. Some of these limitations may be circumvented by compartmentalizing the catalyst within a protein environment.[2,3]

In biology, catalytic cofactors are often protected from the surrounding media by scaffolding within a protein. Borrowing from this methodology, homogeneous catalysts can be anchored into a protein to afford artificial metalloenzymes (ArMs). ArMs may combine advantageous features of organometallic and enzymatic catalysts, providing a means for designing new-to-nature biocatalysts and incorporating synthetic catalysts into cascades. Using this approach, our group has exploited streptavidin (SAV) as a scaffold. These SAV-based ArMs have been optimized to catalyze a variety of organic transformations, summarized in previous reviews.[4−6] Building on this experience, recent work has focused on addressing new challenges: (i) the creation of new cascades, (ii) mimicking cross-regulation by combining ArMs with enzymes, and (iii) directed evolution of ArMs. By building upon these efforts in our future work, our ultimate aim is to create new biocatalytic networks and metabolic pathways *in vivo*.

## 2. ARTIFICIAL METALLOENZYME-DRIVEN ENZYMATIC CASCADES

Cascades involve the combination of two or more concomitant reactions in a single vessel without isolation of intermediates.[7,8] Although cascades are less common in synthetic chemistry, Nature relies on cascades to produce its metabolites. This feat is achieved by enzymes that have evolved to operate in complex mixtures. One advantage of enzymes is that the active site is often protected by the surrounding amino acids. This prevents undesired cross-reactivity or catalyst poisoning. We reasoned that to engineer cascades, SAV-based ArMs may provide an attractive tool. Protecting a catalyst upon incorporation within SAV reduces unwanted side reactions and prevents inhibition.[9]

In our previous Accounts,[5,6] we summarized our efforts toward the development of an artificial transfer hydrogenase for the reduction of imines (ATHase). The cofactor was composed of a $d^6$-piano-stool complex bearing an amino-sulfonamide or aminoamide ligand. These ATHases required molar concentrations of formate, precluding their use *in vivo*. With our aim of developing *in vivo* cascades, we set out to identify a biocompatible hydride source.

### 2.1. An NADPH-Dependent Artificial Transfer Hydrogenases for Multienzymatic Cascades

Inspired by Nature, we selected the $NAD(P)^+$/NAD(P)H couple (and mimics thereof) and evaluated their compatibility with ATHases based on the biotin−streptavidin technology.[10] Initial studies focused on $NAD^+$ mimics, which were shown to act as hydride source with ene-reductases from the Old Yellow Enzyme (OYE) family.[11] A two-enzyme cascade was assembled by combining an ATHase with an ene-reductase.[10,12] By fine-tuning the reaction conditions to minimize the reduction of the enoate by the ATHase,[13] the $NAD^+$ mimic could be recycled by the ATHase using formate as a terminal



DOI: 10.1021/acs.accounts.8b00618
*Acc. Chem. Res.* 2019, 52, 585−595

**Scheme 2. Temporally Programmed Reduction of Enrofloxacin**[a]

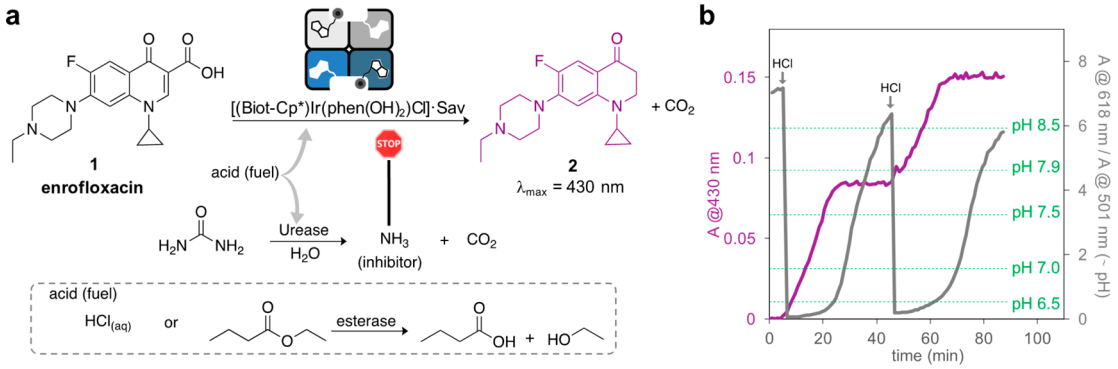


[a](a) Both the ATHase and urease are reversibly inhibited at basic pH. The activity of the urease leads to inhibition of the ATHase, which is restored by acidification, acting as fuel to drive both reactions. (b) Reaction progress (violet) as a function of pH. Adapted from ref 16. Copyright 2017 John Wiley & Sons.

**Scheme 3. Engineering a Third Coordination Sphere around Biotinylated Metal Cofactors by Inclusion within Ferritin**[a]

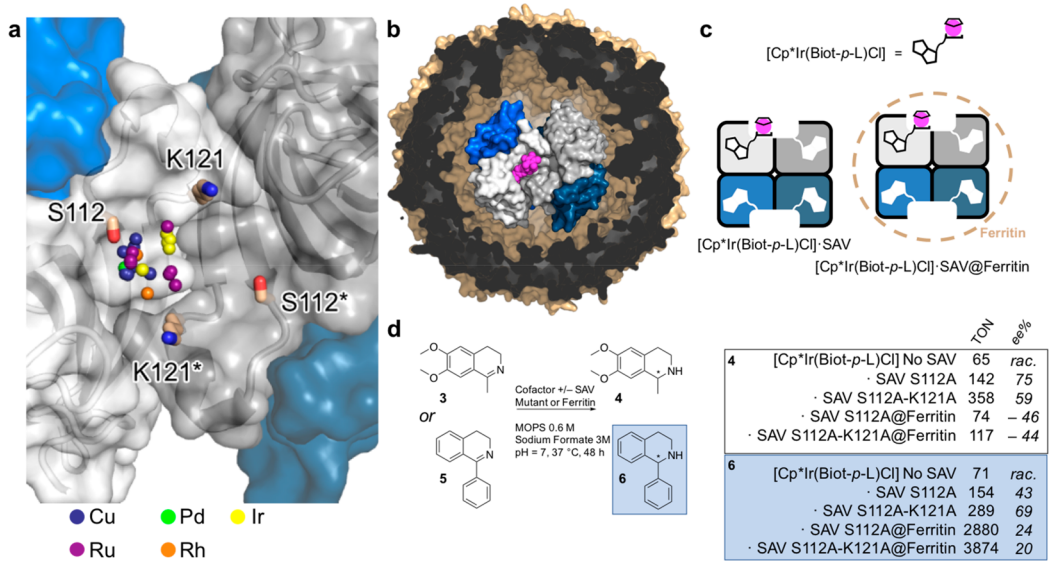


[a](a) Metal distribution of SAV-based ArMs from X-ray. (homotetrameric SAV is displayed as surface, residues S112 and K121 of adjacent SAV monomers forming the biotin-binding vestibule are highlighted in tan; the metals from the biotinylated Ir (yellow, PDB codes 6GMI, 6ESS, 6ESU, 4OKA, and 3PK2), Rh (orange, PDB codes 4GJV and 4GJS), Ru (magenta, PDB codes 6FH8, 5F2B, 5IRA, 2QCB, and 2WPU), Cu (blue, PDB codes 5VKX, 5VL5, 5VL8, 5WBA, 5WBB, 5WBD, 6ANX, 5WBC, 5K67, 5K68, and 5L3Y) and Pd (green, PDB code 5CSE) cofactors are represented by spheres (only one metal per SAV dimer displayed). (b) Slice through the docked structure of [Cp*Ir(Biot-*p*-L)Cl]·SAV (PDB code 3PK2, dimensions 4.5 nm × 5.5 nm × 5.1 nm) encapsulated within ferritin (slice through the surface display (brown shell), PDB code 5C6F). (c) Cartoon representation for [Cp*Ir(Biot-*p*-L)Cl] and ATHase (see Scheme 1 for details). (d) Results of ATHase encapsulated within ferritin. Positive ee, (*R*)-products; negative ee, (*S*)-products.

reductant. The resulting cascade led to the production of cyclic ketones and lactones in high ee (91−93%), Scheme 1a.

We hypothesized that it may be possible to utilize NAD(P)H as a hydride source for the ATHase. For the regeneration of $NADP^+$, we selected glucose dehydrogenase (GDH), an enzyme that converts glucose into gluconolactone, thereby reducing $NADP^+$ to NADPH. To identify the most suitable biotinylated $d^6$-piano-stool complex that accepts a hydride from NADPH, we screened bidentate ligands in combination with either Rh(III) or Ir(III) bearing a biotinylated cyclopentadienyl moiety (Biot−Cp*, Scheme 1b). This allowed us to screen bidentate ligands without biotinylating each ligand prior to screening.[14] Among the 27 bidentate ligands tested, 4,7-dihydroxy-1,10-phenanthroline ($phen(OH)_2$) was the best candidate for the reduction of 1-methyl-3,4-dihydroisoquinoline (MDQ) to 1-methyl-1,2,3,4-tetrahydroisoquinoline (MTQ), Scheme 1c.[15] An enzyme cascade was assembled by combining GDH and the ATHase, enabling reduction of MDQ using glucose as reductant. The performance of the ATHase was fine-tuned by screening a focused library of SAV mutants: [(Biot−Cp*)Ir($phen(OH)_2$)-Cl]·SAV K121R displayed a 5-fold higher turnover compared to WT SAV ATHase. To upgrade the enantioselectivity (<20% ee in favor of (*R*)-MTQ), an (*S*)-selective monoamine oxidase (MAO) was added to the cascade. A catalase (from bovine liver) ensured the rapid disproportionation of $H_2O_2$ produced by the MAO. With this four-enzyme cascade, full conversion with >99% ee was achieved, using only two equivalents of glucose.



DOI: 10.1021/acs.accounts.8b00618
*Acc. Chem. Res.* 2019, 52, 585−595

**Scheme 4. Artificial Metalloenzyme Upregulates a Gene Circuit in Mammalian Cells**[a]

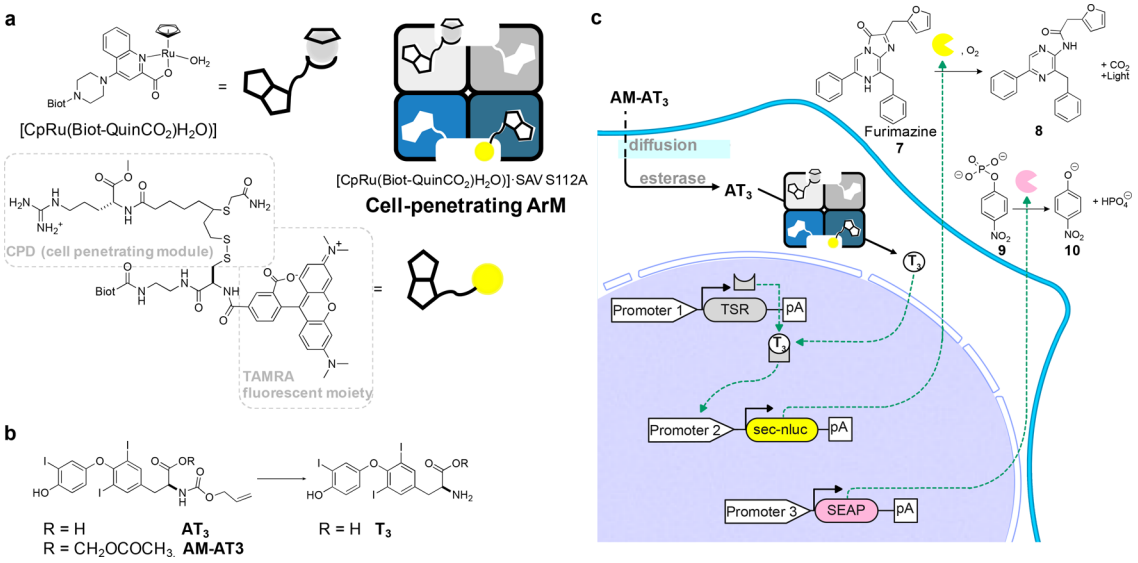


[a](a) The catalyst [CpRu(Biot-Quin$CO_2$)$H_2O$] is combined within SAV with a biotinylated cell-penetrating disulfide CPD equipped with a fluorescent reporter (TAMRA). The cell-penetrating ArM enters the designer HEK-293T cell by covalent-mediated disulfide exchange.[27] (b) The doubly-caged hormone AM-$AT_3$ is hydrolyzed to $AT_3$ by endogeneous esterases. The *O*-allylcarbamate moiety is hydrolyzed *in vivo* by the cell-penetrating ArM to afford $T_3$. (c) The designer HEK-293T cells are equipped with a gene circuit to respond to the $T_3$-hormone, leading to the bioluminescent production of **8** from furimazine. The cell's viability is monitored by the formation of *p*-nitrophenolate produced by a constitutively expressed alkaline phosphatase. Adapted with permission from ref 22. Copyright 2018 Nature Publishing Group.

### 2.2. Enzymatic Regulation of a pH-Programmed ATHase

Metabolic pathways are tightly (cross-)regulated by enzymes that balance the equilibrium of a myriad of reactions required to sustain life. *In vivo*, metabolic pathways are responsive to chemical and physical stimuli. A pathway can be turned on or off to provide cells with necessary resources on demand, limiting the waste of precious metabolic resources. Engineering cross-regulated pathways is challenging but provides a mechanism for regulating catalysis. To address this challenge, we designed a reversible pH-trigger for an ATHase.[16] The activity of the ATHase [(Biot−Cp*)Ir(phen$(OH)_2$)Cl]·SAV K121R is regulated by urease in a pH-responsive fashion, mimicking cross-regulated networks.[16] Enrofloxacin (**1**) was selected as substrate as, upon reduction and decarboxylation, the yellow ketone **2** is produced, which can be monitored spectrophotometrically (Scheme 2a).

Initial studies revealed that the reduction of enrofloxacin by the ATHase [(Biot−Cp*)Ir(phen$(OH)_2$)Cl]·SAV K121R exhibits pH-dependent behavior and proceeds under acidic but not basic conditions. Restoration of ATHase activity is observed upon addition of HCl (pH < 6.0) to a stalled alkaline solution. We reasoned that the pH of the solution may be regulated by urease (from *Canavalia ensiformis*) that hydrolyzes urea to $NH_3$ and $CO_2$, leading to alkalization. Compartmentalization of the cofactor within SAV is essential for both enzymes to coexist: in the absence of SAV, both [(Biot−Cp*)Ir(phen$(OH)_2$)H] and urease suffer from inactivation.

An ATHase and urease mixture containing their respective substrates (urea and enrofloxacin) was prepared at pH = 9. Upon lowering the pH to below 6.5, the two enzymes are activated; both the pH and the formation of **2** can be monitored. The formation of **2** is observed in the acidic regime, but gradual increase in pH caused by the production of ammonia inhibits the reaction above pH ∼ 7. Addition of HCl readily restores both enzymatic activities (Scheme 2b).

The addition of HCl can be circumvented by incorporating an esterase. We envisioned that ethyl butyrate could act as a dormant activator, as it is converted to butyric acid by an esterase (Scheme 2a). As predicted, addition of an esterase to a mixture at pH > 8 consisting of [(Biot−Cp*)Ir(phen$(OH)_2$)-H]·SAV K121R, urease, enrofloxacin, urea, and ethyl butyrate causes a pH decrease, and product formation is detected when an acidic pH is reached. Product formation continues until basic pH is reached.

## 3. COMPARTMENTALIZATION OF ARTIFICIAL METALLOENZYMES IN MORE COMPLEX STRUCTURES

Interactions between the protein and the substrate lead to precise positioning and rapid turnover. From the >20 structurally characterized SAV-based ArMs, the cofactor resides in a narrow dispersion, tweezed between S112 and K121 SAV residues (Scheme 3a). These two residues are often our prime choice for genetic optimization. Despite the undeniable power of this methodology, it does not allow for large perturbations of the ArM's active site owing to the rigidity of the protein scaffold and shallow topology of the biotin binding vestibule (Scheme 3a). In efforts to engineer a more buried active site, we encapsulated an ArM within a protein host to provide the cofactor with a third coordination sphere: the biotinylated ligand and SAV providing the first- and second-coordination spheres, Scheme 3b.

### 3.1. Ferritin as a Tertiary Coordination Sphere

The ferritin family of iron-storage proteins have long been exploited for biotechnological applications.[17] Ferritin comprises 24 monomers that form a ∼7−8 Å spherical cage, which encapsulate, store, and traffic ∼2400 Fe atoms (as Fe/OH/$PO_4$).[17] The reversible formation of apoferritin is achieved upon acidification and neutralization. The encapsulation of a



DOI: 10.1021/acs.accounts.8b00618
Acc. Chem. Res. 2019, 52, 585−595

commensurate cargo is achieved upon refolding ferritin in the presence of the cargo.

We incorporated [Cp*Ir(Biot-*p*-L)Cl]·SAV into apoferritin to probe the effect of ferritin on ATHase activity (Scheme 3d).[18] Access of the protonated substrates **3** or **5** to the ATHase was facilitated by the ferritin 3-fold channels that direct cationic substrates to the interior. The encapsulation of the [Cp*Ir(Biot-*p*-L)Cl]·SAV@ferritin altered product distribution and catalytic performance. In the absence of ferritin, [Cp*Ir(Biot-*p*-L)Cl]·SAV S112A leads to the (*R*)-**4** (75% ee and 142 TON). In contrast, [Cp*Ir(Biot-*p*-L)Cl]·SAV@ferritin affords preferentially (*S*)-**4**. For the most active ATHase, [Cp*Ir(Biot-*p*-L)Cl]·SAV S112A–K121A,[19] encapsulation enhances the TON for substrate **6** (TON = 289 vs 3874 for the free and encapsulated ATHases, respectively). These data highlight the influence the tertiary coordination sphere on the performance of ArMs. Failure to structurally characterize [Cp*Ir(Biot-*p*-L)Cl]·SAV@ferritin by X-ray points toward a high degree of disorder of the ATHase within ferritin. A crystal structure of ferritin (PDB 5C6F)[20] allowed us to model [Cp*Ir(Biot-*p*-L)Cl]·SAV@ferritin (Scheme 3b).

### 3.2. Artificial Metalloenzyme That Regulates a Gene Switch in Mammalian Cells

Whole-cell catalysis has received increasing attention as it offers the possibility to combine abiotic reactions with metabolic pathways. Artificial metalloenzymes may provide versatile tools toward this endeavor. Although several examples involving organometallic catalysis within *E. coli* or mammalian cells have been reported,[21] rarely is there a productive cooperation between the cellular environment and the abiotic reaction that leads to activation of cellular function.

We thus set out to upregulate the expression of a reporter protein in response to an ArM (Scheme 4). The ArM produces a bioactive molecule that triggers the transcription of a gene that can be visualized by the production of a bioluminescent marker. Several factors need to be addressed to ensure the orchestration of this cascade: (i) efficient uptake of ArMs by mammalian cells and subsequent monitoring of ArM localization (Scheme 4a); (ii) engineering of a gene switch that is regulated by the product of the ArM-catalyzed reaction, resulting in (iii) a luminescent readout (Scheme 4c).[22]

(i) Inspired by Meggers' ruthenium catalyst for uncaging of an *O*-allyl carbamate *in vivo*,[23] we synthesized a biotinylated analog Biot-Quin$CO_2$ for assembly with SAV. *In vitro* genetic optimization led us to select [CpRu(Biot-Quin$CO_2$)$H_2O$]·SAV S112A for the *O*-allyl carbamate cleavage of $AT_3$. To overcome modest cellular uptake of related organometallic complexes,[24,25] we combined it with a cell-penetrating module. Thanks to the homotetrameric nature of SAV, we coassembled [CpRu(Biot-quin$CO_2$)$H_2O$] with a biotinylated cell-penetrating moiety. We selected a cell-penetrating poly(disulfide) (CPD), developed by Matile.[26] The CPD contains a fluorescent TAMRA moiety that allows real-time monitoring of the cellular uptake and distribution of the fully assembled ArM. To favor the uptake of the *O*-allylcarbamate-caged thyroid hormone $AT_3$, we esterified it to AM-$AT_3$ (these are readily saponified by endogeneous esterases in mammalian cells).

(ii) The HEK-293T cells were engineered with a $T_3$-responsive gene switch, consisting of genes encoding a synthetic $T_3$-thyroid hormone receptor (TSR) and a Gal4-specific operator sequence under the control of a minimal promoter that induces the expression of a secreted nanoluc (sec-nluc), a bioluminescence reporter. In the presence of $T_3$, the TSR recruits coactivators, triggering histone acetylation to initiate sec-nluc expression. The last step can be monitored by the luminescent conversion of furimazine **7** into product **8**. To highlight cell-viability, an alkaline phosphatase (SEAP) was coexpressed constitutively, leading to the formation *p*-nitrophenolate **10** by hydrolysis of *p*-nitrophenylphosphate (**9**, Scheme 4).

(iii) The HEK-293T cells, transfected with the $T_3$-responsive gene switch, were treated with [CpRu(Biot-Quin$CO_2$)$H_2O$]·SAV S112A. Introduction of the ArM caused an increase in fluorescence as revealed by confocal microscopy and flow cytometry, confirming the ArM's uptake. After incubation and washing, the substrate AM-$AT_3$ was added. The luminescence caused by the gene switch was significantly higher in the presence of [CpRu(Biot-Quin$CO_2$)$H_2O$]·SAV S112A than either with the free cofactor or with no cofactor at all. The ArM devoid of its CPD moiety also gave much lower luminescence. These observations confirm that only cell-penetrating ArMs lead to the uncaging of $AT_3$ *in vivo*, highlighting the importance of membrane permeability. The constitutive expression of an alkaline phosphatase allowed us to monitor the viability of the engineered HEK-293T cells throughout the entire process.

## 4. COMPARTMENTALIZATION AND SURFACE DISPLAY OF ArMS: VERSATILE PLATFORMS FOR DIRECTED EVOLUTION OF ArMS IN LIVING CELLS

### 4.1. Introduction

With the goal of optimizing ArMs through directed evolution, we sought to create a screening platform for ArM activity. Although some catalysts are active *in vivo*, most notably the [CpRu$L_3$]-based systems developed by Meggers,[23−25,28] many precious-metal catalysts are irreversibly poisoned in the cell.[29−31] This deactivation is primarily caused by thiols, most notably glutathione.[31] Previous work with cell-free extracts revealed that diamide oxidizes glutathione, preventing poisoning of iridium catalysts.[31] Implementation of this diamide strategy allowed for optimization by directed evolution of an artificial imine reductase, using cell free extracts.[32] The scope of this strategy, however, is limited because (i) diamide is incompatible with some catalysts and (ii) the method is significantly more laborious than traditional *in vivo* evolution methods, limiting the number of variants that can be practically screened. Alternatively, sequestration of ArMs into chemically distinct compartments offers the opportunity to minimize catalyst poisoning. Two convenient methods of compartmentalization are available for *E. coli*: periplasmic secretion and surface display. Each of these methods presents advantages and disadvantages, Scheme 5.

Unlike the cytoplasm, the periplasm is slightly oxidizing and contains significantly less glutathione (GSH).[34] In addition, GSH in the periplasm exists mostly in it oxidized form, GSSG, which is less deleterious for both ruthenium and iridium catalysts.[29,31] Surface display leads to anchoring of the protein to the outer membrane, significantly reducing exposure to thiols.

In addition to sequestering the catalyst, it was posited that these methods might afford higher access of the substrate and the abiotic cofactor required for ArM assembly. To accumulate in the cytoplasm, the cofactor must transit through the outer



DOI: 10.1021/acs.accounts.8b00618
*Acc. Chem. Res.* 2019, 52, 585−595

**Scheme 5. Strategies for Compartmentalization of ArMs in *E. coli*[a]**

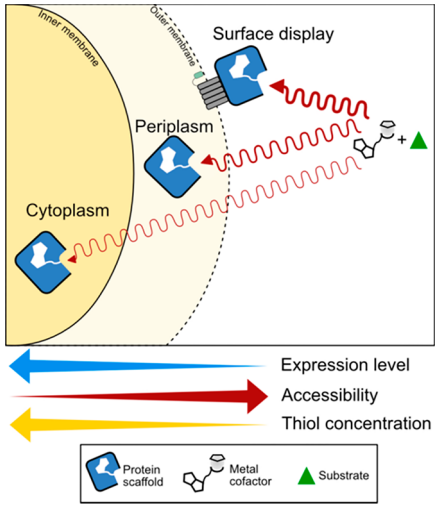


[a]The ArM scaffolds (blue, only one monomer displayed) can be localized in the cytoplasm, in the periplasm, or on the surface. Cytoplasmic expression results in high protein expression but reduces accessibility of the substrate and metal cofactor. Additionally, the cytoplasmic environment is rich in thiols. In contrast, surface display of the ArM scaffold decreases expression level but favorably increases cofactor and substrate accessibility and decreases exposure of the ArM to thiols. Catalysis within the periplasm provides a good compromise in terms of expression level, accessibility, and thiol concentration. Adapted with permission from ref 33. Copyright 2016 Academic Press.

membrane and the less-permeable inner membrane of *E. coli*. Exporting the ArM scaffold to the periplasm eliminates the need for the cofactor to cross the inner membrane. Implementing the surface-display method provides even greater accessibility.

Both periplasmic secretion and surface display retain the phenotype–genotype linkage required for directed evolution. With these features in mind, we assessed the utility of both these methods for directed evolution of ArMs.

### 4.2. Directed Evolution of a Metathase Facilitated by Compartmentalization in *E. coli*'s Periplasm

We reported the directed evolution of a periplasm-localized ArM for olefin metathesis (metathase).[29] Although olefin metathesis is ubiquitously used in organic synthesis, there is no equivalent in Nature. Ru-based metathesis catalysts offer auspicious tools for the creation of ArMs because they are water and oxygen tolerant.[35−37] However, Ru-based metathesis catalysts are sensitive to GSH, either in the presence or in the absence of SAV.[30]

To create a periplasm-compartmentalized ArM scaffold, we modified SAV for periplasmic secretion (Scheme 6). This engineered SAV ($SAV^{peri}$) contained a short, nine amino acid, N-terminal peptide sequence (OmpA). Upon secretion by the SEC pathway, the OmpA tag is cleaved providing untagged SAV.[38] Periplasmic fractionation and fluorescent staining confirmed that $SAV^{peri}$ was secreted to the periplasm and maintained its biotin-binding activity.

The biotinylated metathesis cofactor [$RuCl_2$(Biot−NHC)(styr)] consists of a biotin linked to an Hoveyda−Grubbs second-generation catalyst. ICP-OES of cell fractions confirmed that [$RuCl_2$(Biot−NHC)(styr)] diffuses through the outer membrane and accumulates in the periplasm. When $SAV^{peri}$ is present, the concentration of [$RuCl_2$(Biot−NHC)(styr)] in the periplasm increases 3-fold. To examine the activity of the [$RuCl_2$(Biot−NHC)(styr)]·$SAV^{peri}$, the umbelliferone precursor **11** and [$RuCl_2$(Biot−NHC)(styr)] were incubated with cells lacking or expressing $SAV^{peri}$ (Scheme 6b). Cells expressing $SAV^{peri}$ catalyzed the ring-closing metathesis (RCM) reaction of olefin **11** to yield fluorescent umbelliferone (**12**). Quantification of metathase activity was determined by fluorescence. In the absence of $SAV^{peri}$, negligible metathesis activity was observed in cells. Accordingly, the observed reactivity is attributed to the assembled metathase, enabling quantification with minimal background from the unbound [$RuCl_2$(Biot−NHC)(styr)] cofactor. Thus, we implemented a

**Scheme 6. Metathase Compartmentalized in the Periplasm of *E. coli*[a]**

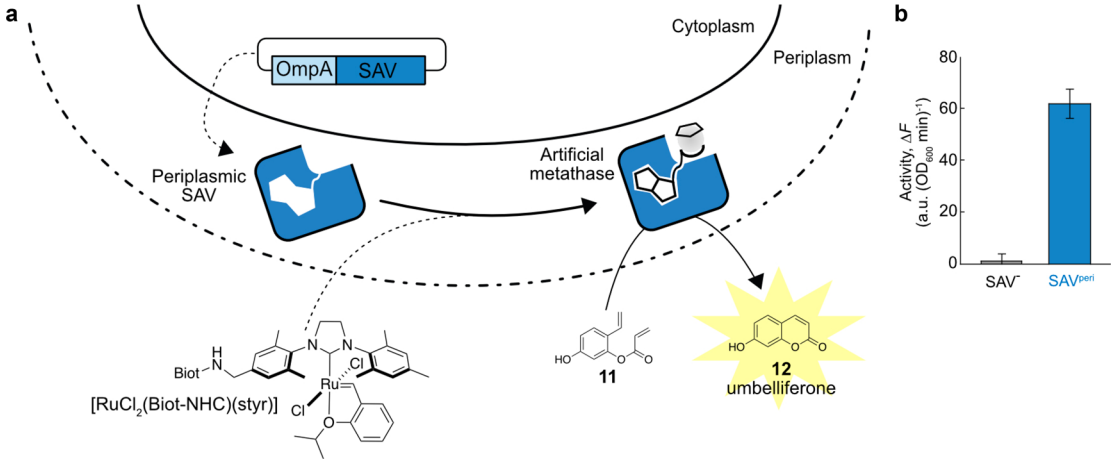


[a](a) Cytoplasmic expression of $SAV^{peri}$ (displayed as a monomer for clarity) is followed by secretion to the periplasm. In the periplasm, the OmpA tag is hydrolyzed, and the homotetrameric $SAV^{peri}$ binds to [$RuCl_2$(Biot−NHC)(styr)], affording the metathase that converts **11** to fluorescent umbelliferone, **12**. (b) *In vivo* activity of the cofactor [$RuCl_2$(Biot−NHC)(styr)] in the absence ($SAV^-$) and presence of $SAV^{peri}$. Adapted with permission from ref 29. Copyright 2016 Nature Research.



DOI: 10.1021/acs.accounts.8b00618
*Acc. Chem. Res.* 2019, 52, 585−595

**Scheme 7. Optimization of a Metathase through Iterative Saturation Mutagenesis**[a]

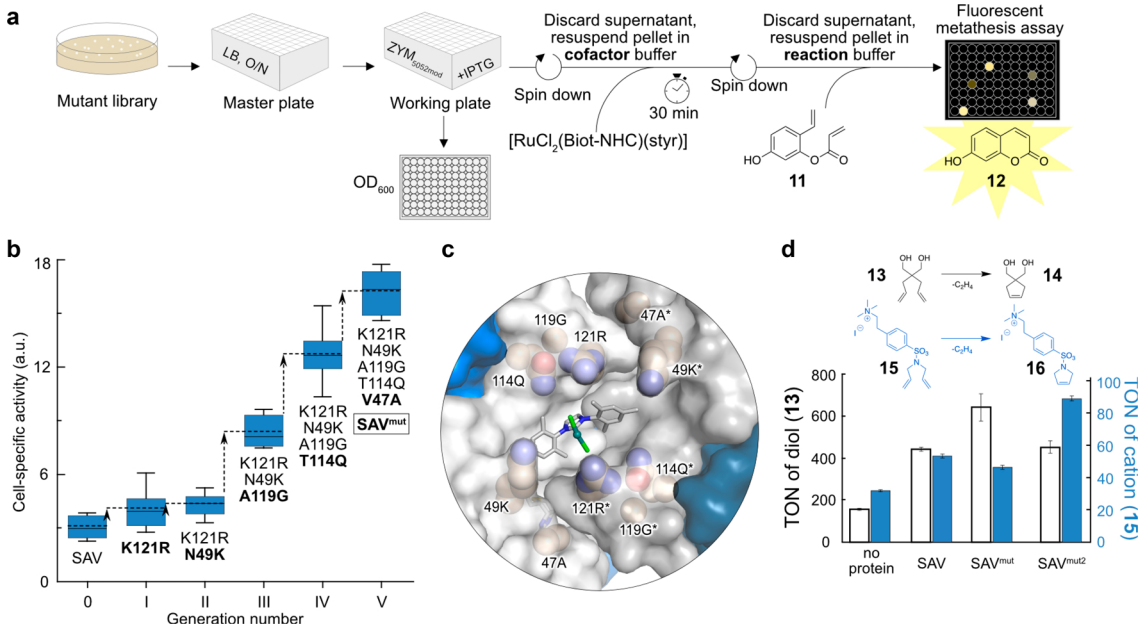


[a](a) Schematic workflow of the fluorescence-based assay for periplasm-localized ArMs. (b) Cell-specific activity allows identifying advantageous mutations obtained during iterative saturation mutagenesis. (c) Structural characterization of the fifth-generation metathase (PDB 5F2B). The asterisks highlight amino acids on the adjacent monomer. (d) Ring-closing metathesis activity of purified metathases towards substrates 2,2-diallyl-1,3-propanediol (**13**) and diallyl-sulfonamide (**15**). Adapted with permission from ref 29. Copyright 2016 Nature Research.

**Scheme 8. Surface Displayed Artificial Deallylase**[a]

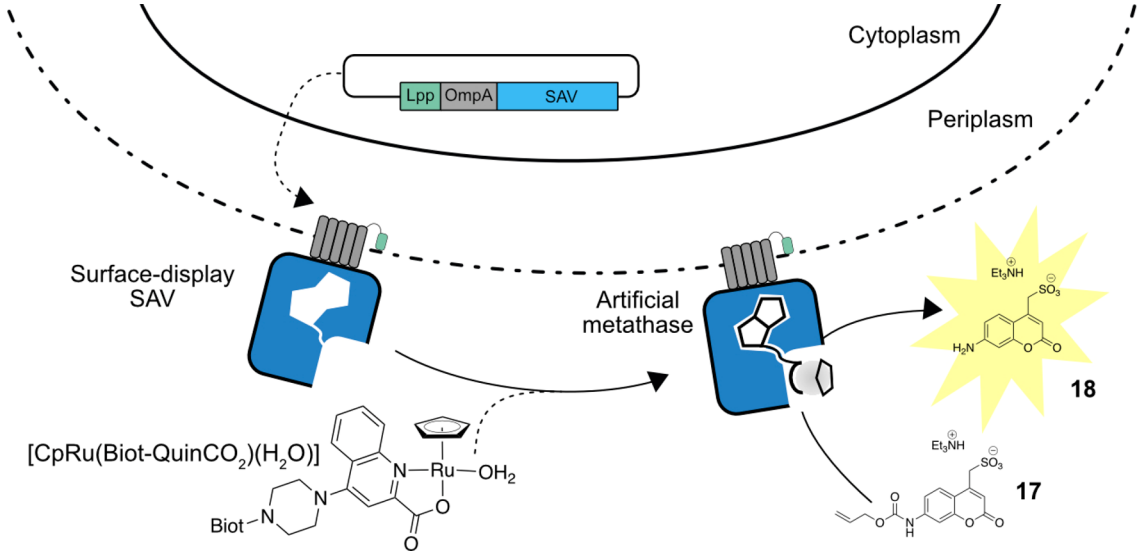


[a]Assembly of the deallylase on the cell surface (single monomer of SAV$^{SD}$ depicted). SAV$^{SD}$ is displayed on the surface enabling facile assembly of the ArM. Once the deallylase is assembled, there is unencumbered access of the allyl-protected substrate **17**. The deallylase converts **17** to the fluorescent product **18**. Adapted with permission from ref 42. Copyright 2018 Royal Society of Chemistry.

protocol for directed evolution based on fluorescent screening of SAV$^{peri}$ mutant libraries in *E. coli* (Scheme 7a).

The screening platform enables rapid 96-well plate analysis of single clones. In this workflow, the DNA library is transformed into chemically competent *E. coli*. For library screening, Top10 cells were selected because they provide the optimal combination of high transformation efficiency and efficient secretion of OmpA-tagged proteins to the periplasm.

DNA libraries were designed for single-site-saturation mutagenesis of the 20 residues closest to the Ru atom based on a docking model of [RuCl$_2$(Biot−NHC)(styr)] with WT SAV. A single mutation at 14 of the 20 proximal residues yielded an advantageous mutant. Iterative saturation mutagenesis[39] at these 14 residues resulted in a mutant with a 5-fold increased activity with **11** using [RuCl$_2$(Biot−NHC)(styr)]·SAV$^{mut}$ (SAV$^{mut}$ = SAV V47A/N49K/T114Q/A119G/K121R).

After directed evolution for metathesis using **11**, we evaluated the substrate scope of the evolved metathase [RuCl$_2$(Biot−NHC)(styr)]·SAV$^{mut}$, using purified SAV$^{mut}$.



DOI: 10.1021/acs.accounts.8b00618
*Acc. Chem. Res.* 2019, 52, 585−595

**Scheme 9. Directed Evolution of an ArM for Deallylation**[a]

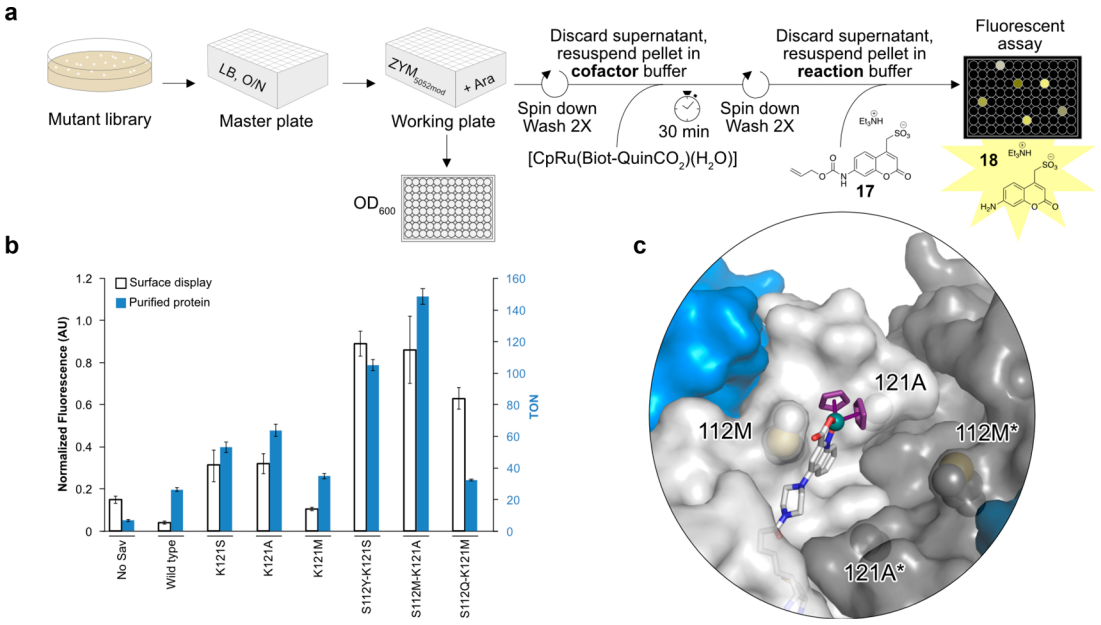


[a](a) Schematic workflow of the fluorescence-based screening for surface-displayed ArMs. (b) Cell-specific activity and TON of purified mutants. (c) Structural characterization by X-ray of the most active ADAse resulting from directed evolution (PDB 6FH8, the Cp moiety, in magenta, as well as the additional solvent ligand were disordered over two positions). Adapted with permission from ref 42. Copyright 2018 Royal Society of Chemistry.

The activity was assessed with two substrates: 2,2-diallyl-1,3-propanediol (**13**) and a cationic diallyl-sulfonamide **15**, Scheme 7d. RCM of **13** yielded the highest turnover with [$RuCl_2$(Biot−NHC)(styr)]·$SAV^{mut}$. Turnover for **15** was higher with WT SAV than with [$RuCl_2$(Biot−NHC)(styr)]·$SAV^{mut}$. We hypothesize that the positively charged 121R residue within the evolved active site may prevent efficient turnover with the cationic substrate.

To identify a metathase for cationic substrates, a second round of directed evolution of $SAV^{mut}$ was conducted with **15**. The positively charged residue K121R of $SAV^{mut}$ was randomized. Screening with **15** was adapted to replace fluorescence detection with LC-MS analysis. The UPLC-MS-based screening revealed that [$RuCl_2$(Biot−NHC)(styr)]·$SAV^{mut2}$ (V47A/N49K/T114Q/A119G/K121L) yielded the highest TON for the cationic substrate. The $SAV^{mut2}$ host performed worse than $SAV^{mut}$ for the neutral substrates **11** and **13**, suggesting that the mutation is only beneficial for the cationic substrate. These results indicate that a rapid fluorescent screening platform can provide a highly valuable starting point for slower LC-MS screening platforms. Gratifyingly, the RCM activity of both the Hoveyda−Grubbs second generation and its water-soluble version (Aquamet) with either substrate **11** or **13** was lower than that obtained in the presence of [$RuCl_2$(Biot−NHC)(styr)]·$SAV^{mut}$.

These results provide a novel method for rapid directed evolution of ArMs in *E. coli*. This method is amenable to "substrate walking" allowing access to diverse substrates, with a limited reoptimization effort. Following the publication of this work, our group has developed an ArM for carbene transfer[40] as well as transfer hydrogenation relying on a self-immolating iminium substrate[41] using a similar periplasmic screening platform.

### 4.3. Directed Evolution of an Allylic Deallylase Facilitated by Surface Display

Surface display also presents a propitious means to protect ArMs from thiols and to increase accessibility of the substrate and metal cofactor. Very recently, we reported a strategy for displaying ArMs on the surface of *E. coli* (Scheme 8).[42] The N-terminal tag for surface display consists of an Lpp peptide (amino acids 1−9) and OmpA (46−159) linked to SAV (Lpp-OmpA-SAV is referred to $SAV^{SD}$ hereafter). Quantitative export of $SAV^{SD}$ to the extracellular space was confirmed by antibody-based staining of cells expressing SAV, $SAV^{peri}$, and $SAV^{SD}$. Although the oligomeric state of $SAV^{SD}$ could not be assessed, other oligomeric proteins form their natural oligomeric state when expressed on the cell surface.[43] Thus, we assume that $SAV^{SD}$ is likely to be a tetramer when expressed on the cell surface.

As a proof of concept, this system was used to evolve an ArM for allylic deallylation (ADAse hereafter) by anchoring [$CpRu(Biot\text{-}QuinCO_2)H_2O$] to $SAV^{SD}$.[42] This [$CpRu(Biot\text{-}QuinCO_2)H_2O$] cofactor was selected because the cofactor catalyzes uncaging at very low catalyst concentrations *in vivo*.[23,24,28]

As a test substrate, the allylcarbamate-protected coumarin **17** was selected. *In vitro*, the [$CpRu(Biot\text{-}QuinCO_2)H_2O$] cofactor catalyzes deprotection of **17** to afford the fluorescent aminocoumarin (**18**). To test the catalyst *in vivo*, cells were incubated with [$CpRu(Biot\text{-}QuinCO_2)H_2O$] in the presence and absence of $SAV^{SD}$. Expression of WT $SAV^{SD}$ resulted in a 1.5-fold increase in production of **18**, which provided an excellent starting point with limited background from unbound catalyst.

To assess the functionality of this platform, iterative saturation mutagenesis was conducted at two sites, (i) K121 and (ii) S112, using the 22-codon trick, previously described by the Reetz laboratory.[44] A fluorescent screening platform,



DOI: 10.1021/acs.accounts.8b00618
Acc. Chem. Res. 2019, 52, 585−595

adapted from the screening platform used for periplasmic screening, was implemented (Scheme 9a). The platform for screening surface-displayed ArMs was amenable to a 96-well format, but washing the cell pellets before and after catalyst addition was required to minimize background.

From the first round of screening with the K121 library, three mutants resulted in significantly higher activity than WT: K121S (7.2-fold), K121A (6.4-fold), and K121M (2.6-fold), Scheme 9b. From these three improved mutants, libraries were created in which position S112 was randomized by saturation mutagenesis.[44] This second round of mutagenesis resulted in additional improvements to the activity compared to WT: S112Y−K121S (25-fold), S112M−K121A (24-fold), and S112Q−K121M (17-fold).

The best SAV mutants were expressed and purified for *in vitro* catalysis. The activity improvements over WT were reduced *in vitro* (Scheme 9b): K121A (2.4-fold), K121S (2.0-fold), K121M (1.3-fold), S112Y−K121S (4.0-fold), S112M−K121A (5.7-fold), and S112Q−K121M (1.2-fold). The origin of these effects may derive from local changes in structure upon surface display or differences in the chemical environment between surface-display and purified SAV samples. Other methods for *in vivo* directed evolution have reported similar effects.[45]

X-ray quality crystals of [CpRu(Biot-Quin$CO_2$)$H_2O$]·S112M−K121A were obtained by crystal soaking the apoprotein with [CpRu(Biot-Quin$CO_2$)$H_2O$] (Scheme 9c). The structure highlights a 112Met−$\pi$ interaction with the quinoline ring of [CpRu(Biot-Quin$CO_2$)$H_2O$] that stabilizes the cofactor. Additionally, a pocket for the quinoline ring is created between the K121A, S112, and L124 from the neighboring SAV monomer.

Using this surface-display screening method, we have shown that ArMs could be evolved with only two rounds of iterative saturation mutagenesis, yielding 25-fold (*in vivo*) and 5.7-fold (*in vitro*) improvements in catalysis. Using the versatile fluorescent screening platform, more complex directed evolution campaigns can be envisioned. To this end, our group is exploring extensive engineering of ArM active sites, including loop insertions.[41,46]

## 5. OUTLOOK

Initiated in 2000, the Ward group has implemented 12 ArMs relying on the biotin−(strept)avidin technology.[4−6] This contribution summarizes our recent efforts toward *in vivo* catalysis and cascade reactions, essential requirements for applications in synthetic biology and artificial metabolism. Toward this goal, both periplasmic secretion and surface display offer exciting avenues to pursue. Future efforts are aimed at tailoring the shallow active site to tackle more challenging reactions that require rigorous control of second coordination sphere interactions between the substrate and the catalyst.

We believe that ArMs hold great promise in two complementary domains: (i) late-stage functionalization of high-added value drugs, whereby catalyst control is highly desirable, and (ii) complementation natural enzymes for synthetic biology applications. In the first domain, ArMs, which are reminiscent of natural enzymes, provide a well-defined secondary coordination sphere that may be an asset in overcoming a substrate's intrinsic reactivity profile. For the latter domain, the *in vivo* combination of natural enzymes with the broad repertoire of homogeneous catalysts will allow us to use microorganisms as test tubes to produce chemicals or fuels. For both applications, directed evolution is an essential tool to identify improved variants.

## AUTHOR INFORMATION


### Corresponding Author

*E-mail: thomas.ward@unibas.ch.

### ORCID

Alexandria Deliz Liang: 0000-0002-9897-2822
Joan Serrano-Plana: 0000-0003-2735-0943
Thomas R. Ward: 0000-0001-8602-5468


### Author Contributions

‡A.D.L., J.S.-P., and R.L.P. made equal contributions.

### Notes

The authors declare no competing financial interest.

### Biographies

**Alexandria Deliz Liang** received her Ph.D. in chemistry from MIT in 2015, where she worked with Stephen J. Lippard. As an NSF postdoctoral fellow, Alexandria worked with Jason Chin (LMB, U.K.). Currently, she is a Marie Skłodowska-Curie Fellow in the laboratory of Thomas Ward, working on alternative ArM scaffolds.

**Joan Serrano-Plana** received his Ph.D. in chemistry from the University of Girona in 2016 under the supervision of Miquel Costas and Anna Company. Thereafter, he joined the group of Thomas Ward as a Marie Skłodowska-Curie Fellow. He is working on the development of ArMs for C−H oxidation.

**Ryan L. Peterson** received his Ph.D. in chemistry from the Johns Hopkins University (JHU) under the guidance of Kenneth D. Karlin in 2013. After graduation, he was a NIH postdoctoral fellow with Valeria Culotta at the JHU Bloomberg School of Public Health. He is currently a postdoctoral fellow in the Ward group, where he is developing new ArM systems.

**Thomas R. Ward** has been active in the field of artificial metalloenzymes since 2000. His current focus is on the directed evolution and valorization of ArMs for late-stage functionalization and synthetic biology purposes.

## ACKNOWLEDGMENTS

T.R.W. thanks the SNF, the NCCR (molecular systems engineering), and the advanced ERC grant (the DrEAM) for generous support. A.D.L. and J.S.-P. thank the EU for Marie Skłodowska-Curie fellowships (H2020-MSCA-IF-2017 and H2020-MSCA-IF-2016).

## REFERENCES


(1) Walsh, C. T.; Moore, B. S. Enzymatic Cascade Reactions in Biosynthesis. *Angew. Chem., Int. Ed.* **2018**, DOI: 10.1002/anie.201807844.

(2) Wörsdörfer, B.; Woycechowsky, K. J.; Hilvert, D. Directed Evolution of a Protein Container. *Science* **2011**, *331*, 589−592.

(3) Engström, K.; Johnston, E. V.; Verho, O.; Gustafson, K. P. J.; Shakeri, M.; Tai, C.-W.; Bäckvall, J.-E. Co-immobilization of an Enzyme and a Metal into the Compartments of Mesoporous Silica for Cooperative Tandem Catalysis: An Artificial Metalloenzyme. *Angew. Chem., Int. Ed.* **2013**, *52*, 14006−14010.

(4) Schwizer, F.; Okamoto, Y.; Heinisch, T.; Gu, Y.; Pellizzoni, M. M.; Lebrun, V.; Reuter, R.; Köhler, V.; Lewis, J. C.; Ward, T. R. Artificial Metalloenzymes: Reaction Scope and Optimization Strategies. *Chem. Rev.* **2018**, *118*, 142−231.




DOI: 10.1021/acs.accounts.8b00618
*Acc. Chem. Res.* 2019, 52, 585−595

(5) Ward, T. R. Artificial Metalloenzymes Based on the Biotin−Avidin Technology: Enantioselective Catalysis and Beyond. *Acc. Chem. Res.* **2011**, *44*, 47−57.
(6) Heinisch, T.; Ward, T. R. Artificial Metalloenzymes Based on the Biotin−Streptavidin Technology: Challenges and Opportunities. *Acc. Chem. Res.* **2016**, *49*, 1711−1721.
(7) Schrittwieser, J. H.; Velikogne, S.; Hall, M.; Kroutil, W. Artificial Biocatalytic Linear Cascades for Preparation of Organic Molecules. *Chem. Rev.* **2018**, *118*, 270−348.
(8) Sperl, J. M.; Sieber, V. Multienzyme Cascade Reactions—Status and Recent Advances. *ACS Catal.* **2018**, *8*, 2385−2396.
(9) Köhler, V.; Wilson, Y. M.; Dürrenberger, M.; Ghislieri, D.; Churakova, E.; Quinto, T.; Knörr, L.; Häussinger, D.; Hollmann, F.; Turner, N. J.; Ward, T. R. Synthetic cascades are enabled by combining biocatalysts with artificial metalloenzymes. *Nat. Chem.* **2013**, *5*, 93.
(10) Okamoto, Y.; Köhler, V.; Paul, C. E.; Hollmann, F.; Ward, T. R. Efficient In Situ Regeneration of NADH Mimics by an Artificial Metalloenzyme. *ACS Catal.* **2016**, *6*, 3553−3557.
(11) Paul, C. E.; Gargiulo, S.; Opperman, D. J.; Lavandera, I.; Gotor-Fernández, V.; Gotor, V.; Taglieber, A.; Arends, I. W. C. E.; Hollmann, F. Mimicking Nature: Synthetic Nicotinamide Cofactors for C=C Bioreduction Using Enoate Reductases. *Org. Lett.* **2013**, *15*, 180−183.
(12) Okamoto, Y.; Ward, T. R. Transfer Hydrogenation Catalyzed by Organometallic Complexes Using NADH as a Reductant in a Biochemical Context. *Biochemistry* **2017**, *56*, 5223−5224.
(13) Heinisch, T.; Langowska, K.; Tanner, P.; Reymond, J.-L.; Meier, W.; Palivan, C.; Ward, T. R. Fluorescence-Based Assay for the Optimization of the Activity of Artificial Transfer Hydrogenase within a Biocompatible Compartment. *ChemCatChem* **2013**, *5*, 720−723.
(14) Betanzos-Lara, S.; Liu, Z.; Habtemariam, A.; Pizarro, A. M.; Qamar, B.; Sadler, P. J. Organometallic Ruthenium and Iridium Transfer-Hydrogenation Catalysts Using Coenzyme NADH as a Cofactor. *Angew. Chem., Int. Ed.* **2012**, *51*, 3897−3900.
(15) Okamoto, Y.; Köhler, V.; Ward, T. R. An NAD(P)H-Dependent Artificial Transfer Hydrogenase for Multienzymatic Cascades. *J. Am. Chem. Soc.* **2016**, *138*, 5781−5784.
(16) Okamoto, Y.; Ward, T. R. Cross-Regulation of an Artificial Metalloenzyme. *Angew. Chem., Int. Ed.* **2017**, *56*, 10156−10160.
(17) Jutz, G.; van Rijn, P.; Santos Miranda, B.; Böker, A. Ferritin: A Versatile Building Block for Bionanotechnology. *Chem. Rev.* **2015**, *115*, 1653−1701.
(18) Hestericová, M.; Heinisch, T.; Lenz, M.; Ward, T. R. Ferritin encapsulation of artificial metalloenzymes: engineering a tertiary coordination sphere for an artificial transfer hydrogenase. *Dalton Transactions* **2018**, *47*, 10837−10841.
(19) Schwizer, F.; Köhler, V.; Dürrenberger, M.; Knörr, L.; Ward, T. R. Genetic Optimization of the Catalytic Efficiency of Artificial Imine Reductases Based on Biotin−Streptavidin Technology. *ACS Catal.* **2013**, *3*, 1752−1755.
(20) Kim, S.; Lee, J.-H.; Seok, J. H.; Park, Y.-H.; Jung, S. W.; Cho, A. E.; Lee, C.; Chung, M. S.; Kim, K. H. Structural Basis of Novel Iron-Uptake Route and Reaction Intermediates in Ferritins from Gram-Negative Bacteria. *J. Mol. Biol.* **2016**, *428*, 5007−5018.
(21) Rebelein, J.; Ward, T. R. In vivo catalyzed new-to-nature reactions. *Curr. Opin. Biotechnol.* **2018**, *53*, 106−114.
(22) Okamoto, Y.; Kojima, R.; Schwizer, F.; Bartolami, E.; Heinisch, T.; Matile, S.; Fussenegger, M.; Ward, T. R. A cell-penetrating artificial metalloenzyme regulates a gene switch in a designer mammalian cell. *Nat. Commun.* **2018**, *9*, 1943.
(23) Völker, T.; Dempwolff, F.; Graumann, P. L.; Meggers, E. Progress towards Bioorthogonal Catalysis with Organometallic Compounds. *Angew. Chem., Int. Ed.* **2014**, *53*, 10536−10540.
(24) Hsu, H.-T.; Trantow, B. M.; Waymouth, R. M.; Wender, P. A. Bioorthogonal Catalysis: A General Method To Evaluate Metal-Catalyzed Reactions in Real Time in Living Systems Using a Cellular Luciferase Reporter System. *Bioconjugate Chem.* **2016**, *27*, 376−382.
(25) Tomás-Gamasa, M.; Martínez-Calvo, M.; Couceiro, J. R.; Mascareñas, J. L. Transition metal catalysis in the mitochondria of living cells. *Nat. Commun.* **2016**, *7*, 12538.
(26) Gasparini, G.; Bang, E.-K.; Molinard, G.; Tulumello, D. V.; Ward, S.; Kelley, S. O.; Roux, A.; Sakai, N.; Matile, S. Cellular Uptake of Substrate-Initiated Cell-Penetrating Poly(disulfide)s. *J. Am. Chem. Soc.* **2014**, *136*, 6069−6074.
(27) Gasparini, G.; Bang, E.-K.; Montenegro, J.; Matile, S. Cellular uptake: lessons from supramolecular organic chemistry. *Chem. Commun.* **2015**, *51*, 10389−10402.
(28) Völker, T.; Meggers, E. Chemical Activation in Blood Serum and Human Cell Culture: Improved Ruthenium Complex for Catalytic Uncaging of Alloc-Protected Amines. *ChemBioChem* **2017**, *18*, 1083−1086.
(29) Jeschek, M.; Reuter, R.; Heinisch, T.; Trindler, C.; Klehr, J.; Panke, S.; Ward, T. R. Directed evolution of artificial metalloenzymes for in vivo metathesis. *Nature* **2016**, *537*, 661.
(30) Mallin, H.; Hestericová, M.; Reuter, R.; Ward, T. R. Library design and screening protocol for artificial metalloenzymes based on the biotin-streptavidin technology. *Nat. Protoc.* **2016**, *11*, 835.
(31) Wilson, Y. M.; Dürrenberger, M.; Nogueira, E. S.; Ward, T. R. Neutralizing the detrimental effect of glutathione on precious metal catalysts. *J. Am. Chem. Soc.* **2014**, *136*, 8928−8932.
(32) Hestericová, M.; Heinisch, T.; Alonso-Cotchico, L.; Maréchal, J.-D.; Vidossich, P.; Ward, T. R. Directed Evolution of an Artificial Imine Reductase. *Angew. Chem., Int. Ed.* **2018**, *57*, 1863−1868.
(33) Jeschek, M.; Panke, S.; Ward, T. R. Periplasmic Screening for Artificial Metalloenzymes. In *Methods in Enzymology*; Pecoraro, V. L., Ed.; Academic Press, 2016; Vol. *580*, Chapter 23, pp 539−556.
(34) Smirnova, G. V.; Oktyabrsky, O. N. Glutathione in Bacteria. *Biochemistry (Moscow)* **2005**, *70*, 1199−1211.
(35) Isarov, S. A. Protein-Polymer Conjugates via Graft-From Ring-Opening Metathesis Polymerization, Masters thesis, Case Western Reserve University, 2015.
(36) Novak, B. M.; Grubbs, R. H. Catalytic organometallic chemistry in water: the aqueous ring-opening metathesis polymerization of 7-oxanorbornene derivatives. *J. Am. Chem. Soc.* **1988**, *110*, 7542−7543.
(37) Sauer, D. F.; Himiyama, T.; Tachikawa, K.; Fukumoto, K.; Onoda, A.; Mizohata, E.; Inoue, T.; Bocola, M.; Schwaneberg, U.; Hayashi, T.; Okuda, J. A Highly Active Biohybrid Catalyst for Olefin Metathesis in Water: Impact of a Hydrophobic Cavity in a *β*-Barrel Protein. *ACS Catal.* **2015**, *5*, 7519−7522.
(38) Cristóbal, S.; de Gier, J. W.; Nielsen, H.; von Heijne, G. Competition between Sec- and TAT-dependent protein translocation in Escherichia coli. *EMBO Journal* **1999**, *18*, 2982−2990.
(39) Reetz, M. T. Laboratory Evolution of Stereoselective Enzymes: A Prolific Source of Catalysts for Asymmetric Reactions. *Angew. Chem., Int. Ed.* **2011**, *50*, 138−174.
(40) Zhao, J.; Bachmann, D. G.; Lenz, M.; Gillingham, D. G.; Ward, T. R. An artificial metalloenzyme for carbene transfer based on a biotinylated dirhodium anchored within streptavidin. *Catal. Sci. Technol.* **2018**, *8*, 2294−2298.
(41) Zhao, J.; Rebelein, J. G.; Mallin, H.; Trindler, C.; Pellizzoni, M. M.; Ward, T. R. Genetic Engineering of an Artificial Metalloenzyme for Transfer Hydrogenation of a Self-Immolative Substrate in Escherichia coli's Periplasm. *J. Am. Chem. Soc.* **2018**, *140*, 13171−13175.
(42) Heinisch, T.; Schwizer, F.; Garabedian, B.; Csibra, E.; Jeschek, M.; Vallapurackal, J.; Pinheiro, V. B.; Marlière, P.; Panke, S.; Ward, T. R. E. coli surface display of streptavidin for directed evolution of an allylic deallylase. *Chemical Science* **2018**, *9*, 5383−5388.
(43) Schüürmann, J.; Quehl, P.; Festel, G.; Jose, J. Bacterial whole-cell biocatalysts by surface display of enzymes: toward industrial application. *Appl. Microbiol. Biotechnol.* **2014**, *98*, 8031−8046.
(44) Kille, S.; Acevedo-Rocha, C. G.; Parra, L. P.; Zhang, Z.-G.; Opperman, D. J.; Reetz, M. T.; Acevedo, J. P. Reducing Codon Redundancy and Screening Effort of Combinatorial Protein Libraries Created by Saturation Mutagenesis. *ACS Synth. Biol.* **2013**, *2*, 83−92.


DOI: 10.1021/acs.accounts.8b00618
*Acc. Chem. Res.* 2019, 52, 585−595

(45) Moore, J. C.; Rodriguez-Granillo, A.; Crespo, A.; Govindarajan, S.; Welch, M.; Hiraga, K.; Lexa, K.; Marshall, N.; Truppo, M. D. Site and Mutation"-Specific Predictions Enable Minimal Directed Evolution Libraries. *ACS Synth. Biol.* **2018**, *7*, 1730−1741.
(46) Pellizzoni, M. M.; Schwizer, F.; Wood, C. W.; Sabatino, V.; Cotelle, Y.; Matile, S.; Woolfson, D. N.; Ward, T. R. Chimeric Streptavidins as Host Proteins for Artificial Metalloenzymes. *ACS Catal.* **2018**, *8*, 1476−1484.



DOI: 10.1021/acs.accounts.8b00618
*Acc. Chem. Res.* 2019, 52, 585−595